

Synthesis and Characterization of [Acridinium][Ni(dmit)₂]₃ and [Phenazinium][Ni(dmit)₂]₃ (dmit = 2-Thioxo-1,3-dithiole-4,5-dithiolate)

Yvonne S. J. Veldhuizen,^{1a} Wilberth J. J. Smeets,^{1b} Nora Veldman,^{1b} Anthony L. Spek,^{*,1b} Christophe Faulmann,^{1c} Pascale Auban-Senzier,^{1d} Denis Jérôme,^{1d} Peter M. Paulus,^{1e} Jaap G. Haasnoot,^{*,1a} and Jan Reedijk^{1a}

Gorlaeus Laboratories, Leiden Institute of Chemistry, Leiden University, P.O. Box 9502, 2300 RA Leiden, The Netherlands, Bijvoet Center for Biomolecular Research and Crystal and Structural Chemistry, Utrecht University, Padualaan 8, 3584 CH Utrecht, The Netherlands, Laboratoire de Chimie de Coordination du CNRS, 205 route de Narbonne, 31077 Toulouse Cedex, France, Laboratoire de Physique des Solides, Associé au CNRS, Centre d'Orsay, Université Paris-Sud, Bâtiment 510, 91405 Orsay Cedex, France, and Kamerlingh Onnes Laboratories, Department of Physics, Leiden University, P.O. Box 9506, 2300 RA Leiden, The Netherlands

Received March 27, 1997[⊗]

Electro-oxidation of a solution of [AcrH][Ni(dmit)₂] (AcrH = acridinium; dmit = 2-thioxo-1,3-dithiole-4,5-dithiolate) yields black crystals of [AcrH][Ni(dmit)₂]₃ (**1**). Black crystals of [PheH][Ni(dmit)₂]₃ (**2**) (PheH = phenazinium) are obtained by slow interdiffusion of solutions of PheHBF₄ and [Bu₄N][Ni(dmit)₂]. Crystals of **1** are monoclinic, of space group *C2/c*, with *a* = 39.124(3) Å, *b* = 6.4777(5) Å, *c* = 20.621(1) Å, *β* = 110.55(1)°, and *Z* = 4. Crystals of **2** are triclinic, of space group *P1*, with *a* = 5.7795(6) Å, *b* = 12.056(1) Å, *c* = 19.041(1) Å, *α* = 71.98(1)°, *β* = 89.47(1)°, *γ* = 77.99(1)°, and *Z* = 1. The crystal structures of the two compounds are very different. In compound **2**, regular stacks of slightly dimerized Ni(dmit)₂ units are found and short S⋯S interactions are found in two dimensions. Compound **1**, however, shows stacks built from trimers of Ni(dmit)₂ units, which are rotated 30° toward each other, forming a "spanning overlapping mode". Short S⋯S interactions are found in all three dimensions. Compound **1** shows a room-temperature conductivity of 45 S·cm⁻¹ and metallic conductivity behavior from room temperature down to 0.4 K. No superconductivity is observed at high pressures of 8 and 13 kbar. Compound **2** shows a room-temperature conductivity of 4 S·cm⁻¹ and semimetallic conductivity behavior from room temperature down to 100 K. The measured conductivity behaviors are in good agreement with the results obtained from band-structure calculations according to a tight-binding model and including Coulomb repulsion.

1. Introduction

The basis for the conducting mixed-valence M(dmit)₂ coordination complexes (M = Ni, Pd, Pt) was formed in 1983 by the electrochemical crystallization of the nonstoichiometric [Bu₄N]₂[Ni(dmit)₂]₂·2CH₃CN by Valade *et al.*² Since then, over 100 conducting coordination compounds based on dmit have been prepared and studied.^{3,4} Among these, a total of six compounds have been shown to possess superconducting properties at low temperatures and under pressure.^{5–10} In

addition, Tajima *et al.*¹¹ in 1993 observed that α-[EDT-TTF]-[Ni(dmit)₂] becomes superconducting at ambient pressure with a value for *T_c* of 1.3 K.

From the Ni(dmit)₂ salts synthesized so far, it has become evident that a (super)conductor can be prepared in combination with an open- as well as with a closed-shell cation. An open-shell cation like TTF introduces an additional conduction path in the compound by the sulfur atoms on the periphery of this molecule. In the case of a closed-shell cation like Me₄N⁺, the size and the shape of the cation only determine the final crystal structure; in this respect Me₄N⁺ is a so-called spectator cation. Both compounds, [TTF][Ni(dmit)₂]₂ and [Me₄N][Ni(dmit)₂]₂, show superconducting properties.^{5,6}

To date, little is known about the factors which govern the packing of cations with the M(dmit)₂ anions. The closed-shell cations used so far are mostly of the tetraalkylammonium type, including the divalent cation 2,2,7,7-tetramethyl-2,7-diazoniaoctane.¹² A few compounds using small saturated and unsaturated ring systems, like *N,N*-dimethylpyrrolidinium and 1,2,3-trimethylimidazolium, have also been synthesized.^{13,14}

* Corresponding authors: J.G.H., all correspondence except that pertaining to the crystallographic studies; A.L.S., correspondence pertaining to the crystallographic studies.

[⊗] Abstract published in *Advance ACS Abstracts*, September 15, 1997.

- (1) (a) Leiden Institute of Chemistry, Leiden University. (b) Utrecht University. (c) Laboratoire de Chimie de Coordination du CNRS. (d) Université Paris-Sud. (e) Department of Physics, Leiden University.
- (2) Valade, L.; Cassoux, P.; Gleizes, A.; Interrante, L. V. *J. Phys. Colloq.* **1983**, *44C3*, 1183.
- (3) Cassoux, P.; Valade, L.; Kobayashi, H.; Kobayashi, H.; Clark, R. A.; Underhill, A. E. *Coord. Chem. Rev.* **1991**, *110*, 115.
- (4) Olk, R.-M.; Olk, B.; Dietzsch, W.; Kirmse, R.; Hoyer, E. *Coord. Chem. Rev.* **1992**, *117*, 99.
- (5) Brossard, L.; Ribault, M.; Bousseau, M.; Valade, L.; Cassoux, P. *C. R. Acad. Sci. Paris, Ser. 2* **1986**, *302*, 205.
- (6) Kobayashi, A.; Kim, H.; Sasaki, Y.; Kato, R.; Kobayashi, H.; Moriyama, S.; Nishio, Y.; Kajita, K.; Sasaki, W. *Chem. Lett.* **1987**, 1819.
- (7) Brossard, L.; Hurdequint, H.; Ribault, M.; Valade, L.; Legros, J.-P.; Cassoux, P. *Synth. Met.* **1988**, *27*, B157.
- (8) Brossard, L.; Ribault, M.; Valade, L.; Cassoux, P. *J. Phys. Fr.* **1989**, *50*, 1521.

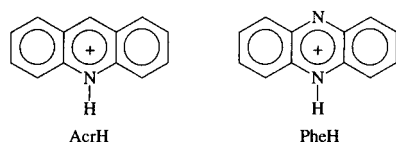
(9) Kobayashi, A.; Kobayashi, H.; Miyamoto, A.; Kato, R.; Clark, R. A.; Underhill, A. E. *Chem. Lett.* **1991**, 2163.

(10) Kobayashi, A.; Bun, K.; Naito, T.; Kato, R.; Kobayashi, A. *Chem. Lett.* **1992**, 1909.

(11) Tajima, H.; Inokuchi, M.; Kobayashi, A.; Ohta, T.; Kato, R.; Kobayashi, H.; Kuroda, H. *Chem. Lett.* **1993**, 1235.

(12) Cornelissen, J. P.; Müller, E.; Vaassens, P. H. S.; Haasnoot, J. G.; Reedijk, J.; Cassoux, P. *Inorg. Chem.* **1992**, *31*, 2241.

Chart 1



In addition to simply combining $M(\text{dmit})_2$ with a large variety of (small) cations, it may be useful to make a series of combinations in which only a small part of the cation has been changed. The effect of such a change on the crystal structure may give more insight into the parameters determining the final crystal structure. Such series have been synthesized among the tetraalkylammonium-type cations by Kato *et al.*,^{5,15} who combined $\text{Ni}(\text{dmit})_2$ with $\text{Me}_y\text{Et}_{4-y}\text{N}^+$ ($y = 0-4$), and in 1994 Pomarède *et al.*¹⁶ published a series of $\text{Ni}(\text{dmit})_2$ compounds with $\text{H}_y\text{Me}_{4-y}\text{N}^+$ ($y = 0-4$). Recently, a series of $\text{Ni}(\text{dmit})_2$ compounds in combination with (methylated) guanidinium was presented.¹⁷⁻²⁰ Guanidinium is a small, planar cation, which crystallized between the separated sheets of $\text{Ni}(\text{dmit})_2$ units with its plane more or less parallel to these sheets. This resulted in an increased overlap of the sulfur orbitals between the sheet and therefore in an increased dimensionality of the compound. Thus it was decided to study the combination of $\text{Ni}(\text{dmit})_2$ with two other planar cations, *viz.* acridinium (AcrH) and phenazinium (PheH) (Chart 1).

Acridine and phenazine are both heterocyclic analogs of anthracene, containing one and two nitrogen atoms in the middle ring, respectively. The cations of nitrogen heterocycles are often synthesized by methylation of the nitrogen atom. Here it was decided to protonate the nitrogen atoms, to keep the shape of the cation as flat as possible. This was expected to improve the packing of the $\text{Ni}(\text{dmit})_2$ units around the cations.

Because of their delocalized π system, AcrH and PheH can be seen as intermediates between typical closed-shell cations such as R_4N ($\text{R} = \text{alkyl}$) and guanidinium and typical open-shell cations such as TTF^+ and EDT-TTF^+ . Besides the crystallization between two-dimensional layers of $\text{Ni}(\text{dmit})_2$ units, the formation of segregated stacks of cations or the intercalation of cations between $\text{Ni}(\text{dmit})_2$ units may therefore also be expected. Such an intercalation was seen, for instance, in the 1:1 combination of $\text{Ni}(\text{dmit})_2$ with *N*-methylquinolinium.²¹

In this paper are reported the syntheses, the crystal structures, and the conducting properties of $[\text{AcrH}][\text{Ni}(\text{dmit})_2]_3$ (**1**) and

$[\text{PheH}][\text{Ni}(\text{dmit})_2]_3$ (**2**). The conducting properties are theoretically analyzed by calculation of the band structures. A preliminary report of this study has been published elsewhere.²²

2. Experimental Section

2.1. Synthesis of $[\text{AcrH}][\text{Ni}(\text{dmit})_2]_3$. (a) **Acridinium Tetrafluoroborate.** A 5 mmol amount of acridine (Fluka AG) was dissolved in approximately 25 mL of diethyl ether. A small excess of tetrafluoroboric acid (~54% in diethyl ether) was added dropwise. The yellow precipitate was filtered off, washed with diethyl ether, and dried in air. Infrared spectroscopy showed the presence of tetrafluoroborate. The salt was used without further purification.

(b) **$[\text{AcrH}][\text{Ni}(\text{dmit})_2]$.** A 0.25 mmol amount of $[\text{Bu}_4\text{N}][\text{Ni}(\text{dmit})_2]$, prepared by the general method of Steimecke *et al.*,²³ was dissolved in 50 mL of acetone (p.a.) under a dinitrogen atmosphere. A solution of 2.5 mmol of acridinium tetrafluoroborate in 25 mL of methanol (p.a.) was added slowly with stirring, and a green solid precipitated immediately. After 20 min of stirring, the solid was filtered off, washed with methanol, and dried under vacuum. Yield: >95%. Infrared spectroscopy showed the exchange of Bu_4N^+ by AcrH^+ . Elemental analysis (C, H, N) performed by University College, Dublin, Ireland, was in agreement with the molecular formula $\text{C}_{19}\text{H}_{10}\text{NNiS}_{10}$. Anal. Calc (found): C, 36.13 (36.24); H, 1.60 (1.57); N, 2.22 (2.28).

(c) **$[\text{AcrH}][\text{Ni}(\text{dmit})_2]_3$ (**1**).** Single crystals of **1** were obtained by electro-oxidation under a dinitrogen atmosphere. A saturated solution of $[\text{AcrH}][\text{Ni}(\text{dmit})_2]$ was obtained by stirring a 0.015 mmol amount in 30 mL of anhydrous acetonitrile for at least 30 min. After the remaining solid had precipitated, the solution was poured into an H-cell equipped with a fine-porosity frit and two platinum wire electrodes ($\varnothing = 1.0$ mm). A constant current of approximately 0.25 μA was applied, and after 1 week, black crystals could be isolated from the anode.

2.2. Synthesis of $[\text{PheH}][\text{Ni}(\text{dmit})_2]_3$. (a) **Phenazinium Tetrafluoroborate.** A 5 mmol amount of phenazine (Aldrich) was dissolved in approximately 75 mL of diethyl ether. A small excess of tetrafluoroboric acid (~54% in diethyl ether) was added dropwise. The yellow precipitate was filtered off, washed with diethyl ether, and dried in air. Infrared spectroscopy showed the presence of tetrafluoroborate. The salt was used without further purification.

N.B. Addition of a large excess of tetrafluoroboric acid results in the precipitation of a red compound, containing the dication of phenazine.²⁴ However, the yellow monocation returns after washing with diethyl ether and drying in air.

(b) **$[\text{PheH}][\text{Ni}(\text{dmit})_2]_3$ (**2**).** On the basis of the results of the synthesis of **1**, the synthesis of $[\text{PheH}][\text{Ni}(\text{dmit})_2]$ was tried first, followed by electro-oxidation. However, the cation exchange of phenazinium tetrafluoroborate with $[\text{Bu}_4\text{N}][\text{Ni}(\text{dmit})_2]$ resulted in the precipitation of microcrystalline **2** immediately, instead of $[\text{PheH}][\text{Ni}(\text{dmit})_2]$. This could be concluded from infrared spectroscopy, showing a C=C stretching vibration at 1249 cm^{-1} indicating further oxidized $\text{Ni}(\text{dmit})_2$, and elemental analysis, showing an anion:cation ratio of 3. The apparent oxidation of $\text{Ni}(\text{dmit})_2$ by phenazinium agrees with the redox properties of phenazinium described in literature.^{24,25} Therefore, the synthesis of $[\text{PheH}][\text{Ni}(\text{dmit})_2]$ was tried by starting from $\text{dmit}(\text{COPh})_2$ and adding phenazinium tetrafluoroborate as the source of the counterion.²³ This resulted in $[\text{PheH}][\text{Ni}(\text{dmit})_2]$ immediately, instead of the usually obtained $[\text{Ni}(\text{dmit})_2]^{2-}$ compound, again because of the oxidizing properties of phenazinium. However, the solubility of $[\text{PheH}][\text{Ni}(\text{dmit})_2]$ appeared to be very low, resulting in only very small crystals during electro-oxidation, which were not suitable for X-ray structure determination. Therefore it was decided to synthesize single crystals of **2** with the cation-exchange method and slow interdiffusion of solutions, using the oxidizing properties of phenazinium.

- (13) (a) Cornelissen, J. P.; Haasnoot, J. G.; Le Loux, R.; Reedijk, J. *Synth. Met.* **1991**, *42*, 2315. (b) Kobayashi, H.; Kato, R.; Kobayashi, A. *Synth. Met.* **1991**, *42*, 2495. (c) Cornelissen, J. P.; Le Loux, R.; Jansen, J.; Haasnoot, J. G.; Reedijk, J.; Horn, E.; Spek, A. L.; Pomarède, B.; Legros, J.-P.; Reefman, D. *J. Chem. Soc., Dalton Trans.* **1992**, 2911.
- (14) (a) Reefman, D.; Cornelissen, J. P.; Haasnoot, J. G.; De Graaff, R. A. G.; Reedijk, J. *Inorg. Chem.* **1990**, *29*, 3933. (b) Cornelissen, J. P.; Creighton, E. J.; De Graaff, R. A. G.; Haasnoot, J. G.; Reedijk, J. *Inorg. Chim. Acta* **1991**, *185*, 97.
- (15) (a) Kato, R.; Mori, T.; Kobayashi, A.; Sasaki, Y.; Kobayashi, H. *Chem. Lett.* **1984**, 1. (b) Kato, R.; Kobayashi, H.; Kim, H.; Kobayashi, A.; Sasaki, Y.; Mori, T.; Inokuchi, H. *Synth. Met.* **1988**, *27*, B359.
- (16) Pomarède, B.; Garreau, B.; Malfant, L.; Valade, L.; Cassoux, P.; Legros, J.-P.; Audouard, A.; Brossard, L.; Ulmet, J.-P.; Doublet, M.-L.; Canadell, E. *Inorg. Chem.* **1994**, *33*, 3401.
- (17) Veldhuizen, Y. S. J.; Veldman, N.; Spek, A. L.; Faulmann, C.; Haasnoot, J. G.; Reedijk, J. *Inorg. Chem.* **1995**, *34*, 140.
- (18) Veldhuizen, Y. S. J.; Haasnoot, J. G.; Maaskant, W. J. A.; Reedijk, J. *Synth. Met.* **1995**, *70*, 1049.
- (19) Paulus, P. M.; Brom, H. B.; Veldhuizen, Y. S. J.; Maaskant, W. J. A. *Solid State Commun.* **1996**, *97*, 737.
- (20) Veldhuizen, Y. S. J.; Veldman, N.; Lakin, M. T.; Spek, A. L.; Paulus, P. M.; Faulmann, C.; Haasnoot, J. G.; Maaskant, W. J. A.; Reedijk, J. *Inorg. Chim. Acta* **1996**, *245*, 27.
- (21) Cornelissen, J. P.; Creighton, E. J.; De Graaff, R. A. G.; Haasnoot, J. G.; Reedijk, J. *Inorg. Chim. Acta* **1991**, *185*, 97.

- (22) Veldhuizen, Y. S. J.; Haasnoot, J. G.; Reedijk, J. *Synth. Met.*, in press.
- (23) Steimecke, G.; Sieler, H. J.; Kirmse, R.; Hoyer, E. *Phosphorus Sulfur* **1979**, *7*, 49.
- (24) Bailey, D. N.; Hercules, D. M.; Roe, D. K. *J. Electrochem. Soc.* **1969**, *116*, 190.
- (25) Bard, A. J.; Lund, H., Eds. *Encyclopedia of Electrochemistry of the Elements, Organic Section*; Marcel Dekker, Inc.: New York, 1984; Vol. XV, Chapter 2.

Table 1. Crystallographic Data for [AcrH][Ni(dmit)₂]₃ (**1**) and [PheH][Ni(dmit)₂]₃ (**2**)

	1	2
empirical formula	C ₃₁ H ₁₀ NNi ₃ S ₃₀	C ₃₀ H ₉ N ₂ Ni ₃ S ₃₀
fw	1534.49	1535.48
space group	C2/c (No. 15)	P1 (No. 2)
<i>a</i> , Å	39.124(3)	5.7795(6)
<i>b</i> , Å	6.4777(5)	12.056(1)
<i>c</i> , Å	20.621(1)	19.041(1)
α , deg	90	71.98(1)
β , deg	110.55(1)	89.47(1)
γ , deg	90	77.99(1)
<i>V</i> , Å ³	4893.4(5)	1231.8(2)
<i>Z</i> , formula units	4	1
<i>D</i> _{calcd.} , g·cm ⁻³	2.083	2.070
μ _{calcd.} , cm ⁻¹	24.6	24.4
λ , Å	0.710 73	0.710 73
<i>T</i> , K	150	150
<i>R</i> ₁ ^a , <i>wR</i> ₂ ^b	0.0518, 0.1338	0.0512, 0.1139

$$^a R_1 = \sum |F_o| - |F_c| / \sum |F_o|. \quad ^b wR_2 = [\sum w(F_o^2 - F_c^2)^2 / \sum w(F_o^2)]^{1/2}.$$

A 0.01 mmol amount of [Bu₄N][Ni(dmit)₂] was put in one "leg" of a λ -shaped diffusion cell, and a 0.05 mmol amount of PheHBF₄ was put in the other leg of the cell. After the cell was brought under a dinitrogen atmosphere, approximately 5 mL of acetone (p.a.) was added to the [Bu₄N][Ni(dmit)₂] and approximately 5 mL of methanol (p.a.) was added to the PheHBF₄. After the solids were dissolved, both legs were further filled with solvent until the levels just touched each other so that interdiffusion of the compounds could occur. The formation of **2** started immediately. The black crystals were isolated after a few days, washed with acetone, and dried in air.

2.3. X-ray Data Collection and Structure Determinations.

Crystal data and numerical details of the structure determinations are given in Table 1. Crystals of both compounds (0.03 \times 0.30 \times 0.75 mm for **1** and 0.02 \times 0.25 \times 0.35 mm for **2**) were glued on glass fibers and transferred to an Enraf-Nonius CAD-4T (rotating anode; graphite-monochromated Mo K α radiation) diffractometer for data collection at 150 K. Unit-cell parameters were determined from a least-squares treatment of the SET4 setting angles of 25 reflections and were checked for the presence of higher lattice symmetry.²⁶ All data were collected with the ω -scan mode and were corrected for *Lp* and for the observed linear decay of the intensity control reflections (2.7% for **1** and 1.0% for **2**). Data for both compounds were corrected for absorption using the DIFABS method²⁷ as implemented in PLATON;²⁸ redundant data were merged into a unique dataset. The structures were solved with direct methods (SHELXS86²⁹) followed by subsequent difference Fourier syntheses. The cations in both structures are located on an inversion symmetry site; therefore, the N atom in **1** and the H atom bonded to N in **2** are disordered in a 50:50 ratio. Refinement on *F*² with all unique reflections was carried out by full-matrix least-squares techniques. Hydrogen atoms were introduced on calculated positions and included in the refinement riding on their carrier atoms with isotropic thermal parameters related to the *U*_{eq} of the carrier atoms. All non-hydrogen atoms were refined with anisotropic thermal parameters. Weights were optimized in the final refinement cycles. The *R*₁ values were calculated for reflections with *F*_o > 4 σ (*F*_o). Final difference Fourier maps of **1** and **2** show residual densities in the ranges -0.61 to +0.68 and -0.62 to +0.75 e \cdot Å⁻³ for **1** and **2**, respectively.

Neutral-atom scattering factors and anomalous-dispersion factors were taken from ref 30. All calculations were performed with SHELXL93³¹ and the PLATON package²⁸ (geometrical calculations and illustrations) on a DEC-5000 cluster. Tables 2 and 3 list the final

Table 2. Final Coordinates and Equivalent Isotropic Thermal Parameters for [AcrH][Ni(dmit)₂]₃ (**1**) (Esd's in Parentheses)

atom ^a	<i>x</i>	<i>y</i>	<i>z</i>	<i>U</i> (eq), Å ²
Ni(1)	0.22816(2)	0.53435(11)	0.32583(3)	0.0152(2)
S(1)	0.04581(4)	0.2466(3)	0.27646(8)	0.0279(5)
S(2)	0.10230(4)	0.5688(2)	0.29286(8)	0.0228(4)
S(3)	0.12134(4)	0.1374(2)	0.28868(7)	0.0190(4)
S(4)	0.20012(4)	0.2428(2)	0.31082(7)	0.0172(4)
S(5)	0.17926(4)	0.7072(2)	0.31480(7)	0.0205(4)
S(6)	0.27717(4)	0.3674(2)	0.33330(7)	0.0165(3)
S(7)	0.25617(4)	0.8262(2)	0.34583(7)	0.0181(4)
S(8)	0.35479(4)	0.5130(2)	0.36273(7)	0.0180(4)
S(9)	0.33446(4)	0.9401(2)	0.37298(7)	0.0190(4)
S(10)	0.41126(4)	0.8448(3)	0.39326(8)	0.0283(4)
C(1)	0.08778(15)	0.3152(9)	0.2854(3)	0.0206(17)
C(2)	0.15655(14)	0.3134(9)	0.3008(3)	0.0162(16)
C(3)	0.14745(14)	0.5179(9)	0.3022(3)	0.0187(17)
C(4)	0.30924(14)	0.5561(9)	0.3508(3)	0.0178(14)
C(5)	0.29924(15)	0.7626(9)	0.3558(3)	0.0174(16)
C(6)	0.36947(14)	0.7694(8)	0.3774(3)	0.0171(16)
Ni(2)	1/4	1/4	1/2	0.0187(3)
S(11)	0.06625(5)	-0.0554(3)	0.42917(9)	0.0357(5)
S(12)	0.14364(4)	-0.1537(2)	0.45601(7)	0.0244(4)
S(13)	0.12348(4)	0.2732(2)	0.46477(7)	0.0239(4)
S(14)	0.22226(4)	-0.0421(2)	0.48337(7)	0.0221(4)
S(15)	0.20111(4)	0.4189(2)	0.49326(7)	0.0216(4)
C(7)	0.1088(2)	0.0182(10)	0.4495(3)	0.0244(17)
C(8)	0.1786(2)	0.0261(9)	0.4731(3)	0.0199(16)
C(9)	0.16931(15)	0.2283(9)	0.4772(3)	0.0196(17)
N(1)*	0.01624(14)	0.6332(9)	-0.0316(3)	0.0316(17)
C(10)	0.0177(2)	0.6773(10)	0.0336(3)	0.0307(19)
C(11)	0.0355(2)	0.8582(10)	0.0689(3)	0.0301(17)
C(12)	0.0368(2)	0.8953(12)	0.1345(3)	0.0381(19)
C(13)	0.0204(2)	0.7556(12)	0.1678(3)	0.040(3)
C(14)	0.0027(2)	0.5830(12)	0.1354(4)	0.041(2)
C(15)	-0.0008(2)	0.4593(10)	-0.0678(3)	0.031(2)
C(16)*	0.01624(14)	0.6332(9)	-0.0316(3)	0.0316(17)

^a Starred atom sites have site occupation factor = 0.5. ^b *U*(eq) is one-third of the trace of the orthogonalized **U** tensor.

fractional coordinates and the equivalent isotropic thermal parameters of the non-hydrogen atoms of **1** and **2**, respectively.

2.4. Conductivity Measurements. Conductivity measurements were carried out at ambient pressure using the four-probe method. Three crystals of **1** were measured in the temperature range 300–4 K, and two crystals of **2** were measured in the temperature range 300–100 K. Four gold wires were glued on thin bar-shaped crystals of 0.85 \times 0.07 \times 0.01, 1.21 \times 0.13 \times 0.03, and 0.97 \times 0.03 \times 0.01 mm for **1** and on rectangular elongated plates of 0.93 \times 0.14 \times 0.02 and 1.36 \times 0.14 \times 0.02 mm for **2**.

High-pressure measurements down to 0.4 K were carried out on a sample of compound **1** measured first at 8 and subsequently at 13 kbar. Two more samples of **1** were measured down to 0.4 K at ambient pressure as well. The high pressure was achieved in a clamped CuBe pressure cell using a silicone oil as the pressure medium. All samples were cooled in a ³He refrigerator, which allowed us to reach 0.4 K.

2.5. Band-Structure Calculations. A theoretical analysis of the electronic structures of **1** and **2** was carried out according to the model applied for the series of [Me_{*x*}-guanidinium][Ni(dmit)₂]₂ compounds (*x* = 0, 2, 4, 6) described by P. M. Paulus *et al.*¹⁹ The molecular orbitals of the neutral Ni(dmit)₂ were calculated using the extended Hückel program ICON8,³² with semiempirical parameters taken from McGlynn *et al.* and Ballhausen *et al.*^{33,34} The intermolecular orbital overlap integrals between the HOMO and the LUMO of the Ni(dmit)₂ units

(26) Spek, A. L. *J. Appl. Crystallogr.* **1988**, *21*, 578.

(27) Walker, N.; Stuart, D. *Acta Crystallogr.* **1983**, *A39*, 158.

(28) Spek, A. L. *Acta Crystallogr.* **1990**, *A46*, C34.

(29) Sheldrick, G. M. SHELXS86: Program for crystal structure determination. University of Göttingen, Germany, 1986.

(30) Wilson, A. J. C., Ed. *International Tables for Crystallography*; Kluwer Academic Publishers: Dordrecht, The Netherlands, 1992; Vol. C.

(31) Sheldrick, G. M. SHELXL93: Program for crystal structure refinement. University of Göttingen, Germany, 1993.

(32) Howell, J.; Rossi, A.; Wallace, D.; Haraki, K.; Hoffmann, R. *ICON8 and FORTICON: QCPE Programs for Extended Hückel Calculations*; Department of Chemistry, Indiana University: Bloomington, IN, 1977.

(33) McGlynn, S. P.; Vanquickenborne, L. G.; Konoshita, M.; Carroll, D. G., Eds. *Introduction to Applied Quantum Chemistry*; Holt, Rhinehart and Winston Inc.: New York, 1972.

(34) Ballhausen, C. J.; Gray, H. B., Eds. *Molecular Orbital Theory*; W. A. Benjamin, Inc.: New York, 1964.

Table 3. Final Coordinates and Equivalent Isotropic Thermal Parameters for [PheH][Ni(dmit)₂]₃ (2) (Esd's in Parentheses)

atom	x	y	z	U(eq), ^a Å ²
Ni(1)	0.03543(11)	0.21679(7)	0.44655(4)	0.0143(2)
S(1)	-0.2021(3)	-0.11392(15)	0.80737(8)	0.0270(5)
S(2)	0.1287(2)	-0.06427(14)	0.68627(8)	0.0201(4)
S(3)	-0.3482(2)	0.08375(14)	0.66750(8)	0.0195(4)
S(4)	-0.2652(2)	0.22987(13)	0.51280(7)	0.0171(4)
S(5)	0.2424(2)	0.06986(13)	0.53242(7)	0.0176(4)
S(6)	-0.1705(2)	0.36339(13)	0.35913(7)	0.0177(4)
S(7)	0.3398(2)	0.20208(13)	0.38143(7)	0.0168(4)
S(8)	-0.0464(2)	0.49420(13)	0.20516(8)	0.0218(4)
S(9)	0.4316(2)	0.34837(13)	0.22825(7)	0.0194(4)
S(10)	0.3022(3)	0.54838(15)	0.08946(8)	0.0303(5)
C(1)	-0.1418(9)	-0.0361(5)	0.7255(3)	0.0180(17)
C(2)	-0.1719(8)	0.1187(5)	0.5930(3)	0.0168(16)
C(3)	0.0544(8)	0.0472(5)	0.6015(3)	0.0159(17)
C(4)	0.0227(8)	0.3856(5)	0.2907(3)	0.0174(17)
C(5)	0.2498(9)	0.3137(5)	0.3007(3)	0.0183(17)
C(6)	0.2313(9)	0.4681(5)	0.1691(3)	0.0210(17)
Ni(2)	0	1/2	1/2	0.0142(3)
S(11)	0.2331(2)	0.83336(15)	0.13666(8)	0.0265(5)
S(12)	-0.0986(2)	0.78174(13)	0.25842(7)	0.0176(4)
S(13)	0.3785(2)	0.63783(13)	0.27726(7)	0.0177(4)
S(14)	-0.2156(2)	0.64528(14)	0.41272(7)	0.0171(4)
S(15)	0.3023(2)	0.49118(13)	0.43318(7)	0.0165(4)
C(7)	0.1704(9)	0.7549(5)	0.2195(3)	0.0186(17)
C(8)	-0.0263(8)	0.6703(5)	0.3428(3)	0.0150(16)
C(9)	0.2005(9)	0.6017(5)	0.3526(3)	0.0153(17)
N(1)	0.7144(7)	-0.0436(4)	0.0382(2)	0.0230(14)
C(10)	0.5918(9)	0.0700(5)	0.0350(3)	0.0235(19)
C(11)	0.6847(10)	0.1395(6)	0.0676(3)	0.0304(19)
C(12)	0.5578(11)	0.2533(6)	0.0611(3)	0.036(2)
C(13)	0.6300(9)	-0.1130(5)	0.0059(3)	0.0223(17)
C(14)	0.7563(10)	-0.2278(6)	0.0104(3)	0.0298(19)
C(15)	0.3361(11)	0.2954(6)	0.0220(3)	0.037(2)

^a U(eq) is one-third of the trace of the orthogonalized **U** tensor.**Table 4.** Coordination Bond Distances (Å) and Bond Angles (deg) for [AcrH][Ni(dmit)₂]₃ (1) (Esd's in Parentheses)^a

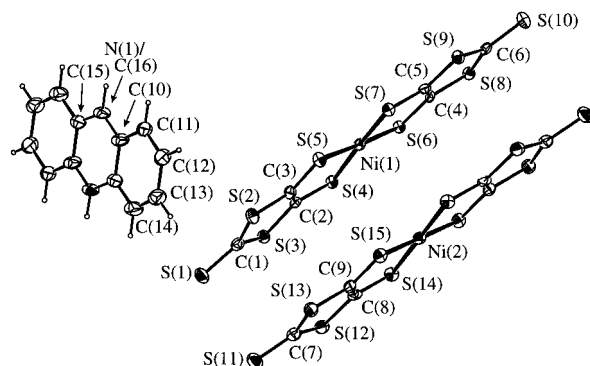
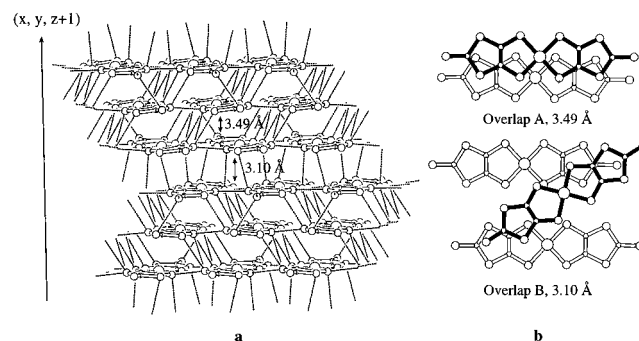
Ni(1)–S(4)	2.1512(16)	Ni(2)–S(14)	2.1481(14)
Ni(1)–S(5)	2.1587(18)	Ni(2)–S(15)	2.1653(16)
Ni(1)–S(6)	2.1593(18)		
Ni(1)–S(7)	2.1512(16)		
S(4)–Ni(1)–S(5)	92.97(6)	S(14)–Ni(2)–S(15)	92.83(6)
S(4)–Ni(1)–S(6)	88.04(6)	S(14)–Ni(2)–S(15) ^a	87.17(6)
S(4)–Ni(1)–S(7)	177.25(6)	S(14)–Ni(2)–S(14) ^a	180
S(5)–Ni(1)–S(6)	177.77(6)		
S(5)–Ni(1)–S(7)	86.41(6)		
S(6)–Ni(1)–S(7)	92.67(6)		

^a Symmetry operation: 1/2 - x, 1/2 - y, 1 - z.

were calculated using the scheme described by Kramer and Roothaan.³⁵ The results were used to calculate the band structures, using a tight-binding model, including a Coulomb repulsion (*U*) of at least the energy difference between the highest LUMO and the lowest HOMO level. The relative conductivity of the compounds was calculated from the bandwidth and the activation energy of the band structures.¹⁹

3. Results

3.1. Descriptions of the Crystal Structures. (a) [AcrH][Ni(dmit)₂]₃ (1). The coordination bond distances and bond angles of **1** are presented in Table 4. The crystallographically independent unit with the labeling scheme used is shown in Figure 1. The structure consists of one and a half independent Ni(dmit)₂ units in a face-to-face orientation and half a cation, which is disordered across the inversion center at the center of

**Figure 1.** The crystallographically independent unit with atomic labeling scheme of [AcrH][Ni(dmit)₂]₃ (1), shown by an ORTEP 50% probability plot (PLATON).**Figure 2.** (a) Sheet of Ni(dmit)₂ units in the *bc* plane of [AcrH][Ni(dmit)₂]₃ (1). (b) Modes of intermolecular overlapping of Ni(dmit)₂ units.

its central ring. The Ni(dmit)₂ units are almost parallel to each other, making an angle of 1.07(4)°. The angle between AcrH and the Ni(dmit)₂ units is 72.8(1)°. The cations form layers between the sheets of Ni(dmit)₂ units, as is commonly found for closed-shell cations in combination with Ni(dmit)₂.

The NiS₄ coordination geometry of Ni(1)(dmit)₂ is slightly distorted from a square-planar toward a tetrahedral configuration, the twist between the planes S(4)–Ni(1)–S(6) and S(5)–Ni(1)–S(7) being 3.43(8)°. Both Ni(dmit)₂ units show rather large deviations from the least-squares planes through all the atoms of the residues for a thionyl sulfur atom, being 0.147(2) Å for S(1) and 0.102(2) Å for S(11), for Ni(1)(dmit)₂ and Ni(2)(dmit)₂, respectively. AcrH is almost perfectly planar. The largest deviation is found for C(15), being 0.013(7) Å.

Figure 2a shows the two-dimensional sheet of Ni(dmit)₂ units which is formed in the *bc* plane of the unit cell. S...S distances shorter than 3.70 Å, the sum of the van der Waals radii,³⁶ are shown by dotted lines. Because of the space group being *C2/c* and the independent Ni(dmit)₂ units lying face-to-face to each other, a rather unusual way of stacking can be seen. In fact, the sheet is built from trimers of Ni(dmit)₂ units, with an average distance of 3.28–3.70 Å from all the atoms of one Ni(dmit)₂ to the least-squares plane through all the atoms of the next Ni(dmit)₂ unit. Within the trimer, a short S...S interaction of 3.552(2) Å is found. The average distance between two trimers (calculated as above) is extremely small, 2.65–3.64 Å, resulting in a shortest S...S interaction of 3.469(2) Å. More important, however, is that the two trimers are rotated approximately 30° toward each other along their stacking axes. The effect is that the upper and lower Ni(dmit)₂ unit of every trimer has short S...S interactions with two Ni(dmit)₂ units of the next trimer.

(35) (a) Kramer, G. J. Ph.D. Thesis, Leiden University, Leiden, The Netherlands, 1988. (b) Roothaan, C. C. J. *J. Chem. Phys.* **1951**, *19*, 1445.(36) Pauling, L. *The Nature of the Chemical Bond*, 2nd ed.; Cornell University Press: Ithaca, NY, 1948.

Table 5. Coordination Bond Distances (Å) and Bond Angles (deg) for [PheH][Ni(dmit)₂]₃ (**2**) (Esds in Parentheses)^a

Ni(1)–S(4)	2.1455(14)	Ni(2)–S(14)	2.1705(14)
Ni(1)–S(5)	2.1457(16)	Ni(2)–S(15)	2.1558(13)
Ni(1)–S(6)	2.1568(16)		
Ni(1)–S(7)	2.1515(14)		
S(4)–Ni(1)–S(5)	92.98(6)	S(14)–Ni(2)–S(15)	92.84(5)
S(4)–Ni(1)–S(6)	87.64(6)	S(14)–Ni(2)–S(14) ^a	180
S(4)–Ni(1)–S(7)	179.22(7)	S(14)–Ni(2)–S(15) ^a	87.16(5)
S(5)–Ni(1)–S(6)	179.22(6)		
S(5)–Ni(1)–S(7)	86.26(6)		
S(6)–Ni(1)–S(7)	93.12(6)		

^a Symmetry operation: $-x, 1 - y, 1 - z$.

The rotation can be seen very clearly in Figure 2b, where the modes of overlap are presented. The rotated overlap is called the “spanning overlapping mode” and has been found previously in two other Ni(dmit)₂ compounds, α -[Et₂Me₂N][Ni(dmit)₂]₂ and [N,N-dimethylpiperidinium][Ni(dmit)₂]₂.^{37,38} Both of these compounds show two-dimensional metallic conducting behavior down to 1.5 K. In addition to the already mentioned intra- and intertrimer interactions, many interstack interactions, of which the shortest is 3.375(2) Å, are present in the structure. However, the shortest S⋯S interaction of all is in the *a* direction of the crystal structure and is 3.361(2) Å. All of these interactions together give this compound a truly three-dimensional character.

(b) [PheH][Ni(dmit)₂]₃ (**2**). Table 5 lists the coordination bond distances and bond angles of **2**. The crystallographically independent unit with the labeling scheme used is shown in Figure 3. As in **1**, the structure consists of one and a half independent Ni(dmit)₂ units in a face-to-face orientation and half a cation, which is disordered across the inversion center at the center of its central ring. The Ni(dmit)₂ units are almost parallel to each other, making an angle of 1.08(5)°. The angle between PheH and the Ni(dmit)₂ units is 86.97(9)°, showing that the cations are positioned with their planes more or less parallel to the sheets of the Ni(dmit)₂ units.

The NiS₄ coordination geometry in Ni(1)(dmit)₂ is hardly distorted from square planar, the twist between the planes S(4)–Ni(1)–S(6) and S(5)–Ni(1)–S(7) being only 0.51(9)°. The largest deviation from the least-squares planes through all of the atoms of the units is rather large for Ni(1)(dmit)₂, being 0.151(2) Å for S(10), and much smaller for Ni(2)(dmit)₂, namely 0.068(2) Å for S(11). The cation is almost completely planar with a largest deviation of only 0.020(5) Å for C(10).

Although the crystallographically independent unit of **2** is quite similar to the independent unit of **1**, the packing of the sheets in the *ab* plane of the crystal structure is quite different. The differences are related to the difference in space group, being *C2/c* for **1** and *P1* for **2**. Figure 4a shows the two-dimensional sheet of Ni(dmit)₂ units in **2** which are formed of Ni(dmit)₂ stacks running parallel to the *b* axis. S⋯S distances shorter than 3.70 Å, the sum of the van der Waals radii,³⁶ are shown by dotted lines and listed in Table S8 of the Supporting Information. One intrastack interaction of 3.602(2) Å is found and several interstack interactions, of which the shortest is 3.4772(18) Å, can be seen in Figure 4a. Despite the planarity of the cation, no short interactions were found in the *c* direction of the crystal structure.

Figure 4b shows the modes of intermolecular overlap of the Ni(dmit)₂ units in the stack. The calculated distances are the

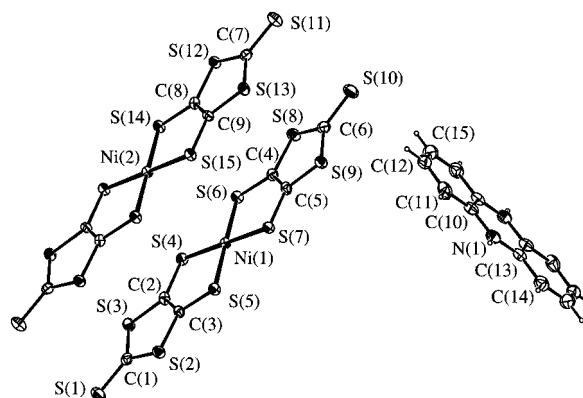


Figure 3. The crystallographically independent unit with atomic labeling scheme of [PheH][Ni(dmit)₂]₃ (**2**), shown by an ORTEP 50% probability plot (PLATON).

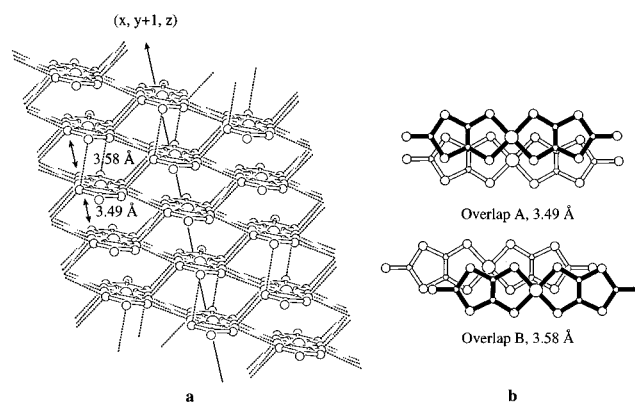


Figure 4. (a) Sheet of Ni(dmit)₂ units in the *ab* plane of [PheH][Ni(dmit)₂]₃ (**2**). (b) Modes of intermolecular overlapping of Ni(dmit)₂ units.

average values of the distances of all atoms of one Ni(dmit)₂ unit to the least-squares plane through all the atoms of the next Ni(dmit)₂ unit. The shift along the short axis of the units only, together with the shorter distance between the units in overlap A, will result in a better overlap of the orbitals in this pair than in the pair of units in overlap B. This usually results in a semiconducting behavior at room temperature.

3.2. Conductivity Measurements. Figure 5a shows that all three crystals of compound **1** have metallic conductivity behavior down to 4 K. The room-temperature conductivity of the crystals is about 45 S·cm⁻¹ and increases to approximately 10³ S·cm⁻¹ at 4 K. No differences in conductivity are observed between the cooling and the heating cycles.

Figure 5b shows that ln(σ) of the crystals of compound **2** decreases with 1/*T*, meaning that the compound shows semiconducting behavior in the whole temperature range. The room-temperature conductivity of the crystals is approximately 4 S·cm⁻¹, and the activation energy is 0.11 eV for the whole temperature range. No hysteresis was observed between the cooling and the heating cycles.

Figure 6 shows the temperature dependence of the resistivity of compound **1** at different pressures. At ambient pressure, the resistivity decreases with the temperature following an S-shaped curve and remains metallic down to 0.47 K. The magneto-resistance measured at $T \approx 1.7$ K and $P = 1$ bar appears to be very weak: $[R(H) - R(0)]/R(0) \approx 10\%$ at $H = 12$ T, in contrast with the quasi-one-dimensional Bechgaard salts.

When a hydrostatic pressure is applied, the conductivity increases linearly at a rate of $[\sigma(P) - \sigma(0)]/\sigma(0) = +15\%/kbar$. The temperature dependence of the resistivity at $P = 8$ and 13 kbar presents the same metallic behavior as for ambient pressure.

(37) (a) Kato, R.; Kobayashi, H.; Kim, H.; Kobayashi, A.; Sasaki, Y.; Mori, T.; Inokuchi, H. *Synth. Met.* **1988**, *27*, B359. (b) Kato, R.; Kobayashi, H.; Kim, H.; Kobayashi, A.; Sasaki, Y.; Mori, T.; Inokuchi, H. *Chem Lett.* **1988**, 865.

(38) Kobayashi, H.; Kato, R.; Kobayashi, A. *Synth. Met.* **1991**, *42*, 2495.

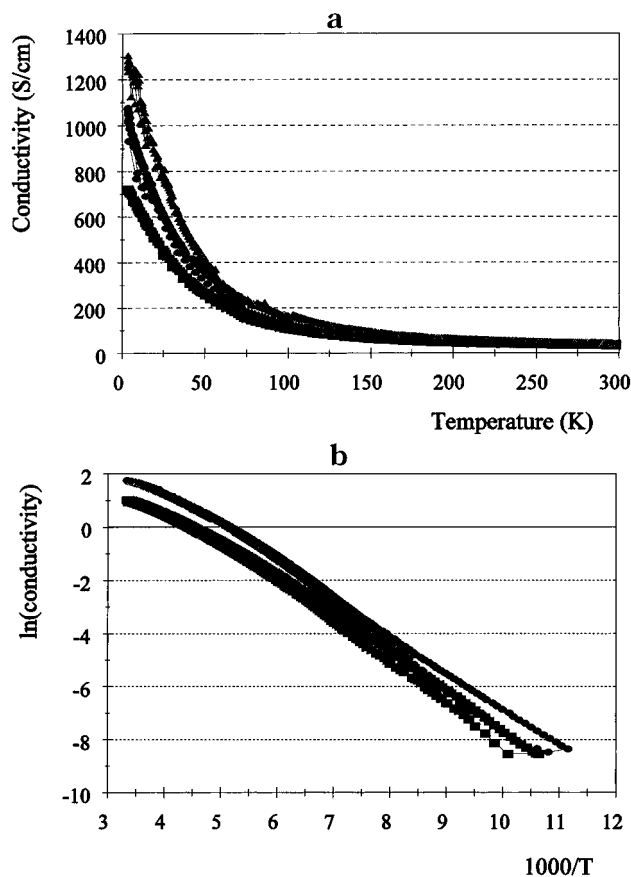


Figure 5. (a) Temperature dependence of the conductivity of [AcrH]-[Ni(dmit)₂]₃ (**1**). (b) Temperature dependence of the conductivity of [PheH][Ni(dmit)₂]₃ (**2**). Different symbols indicate different crystals.

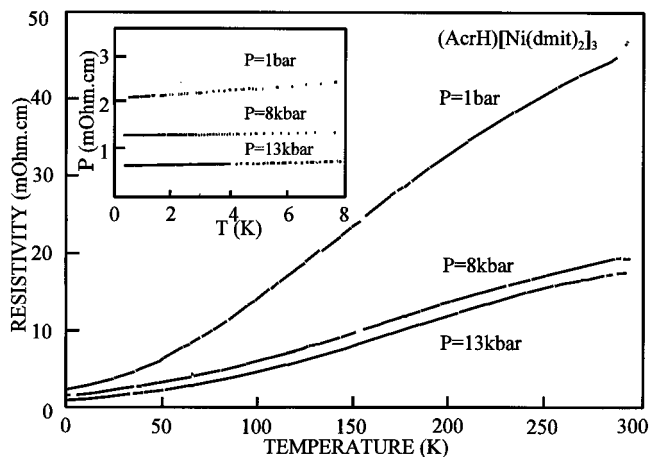


Figure 6. Temperature dependence of the conductivity of [AcrH]-[Ni(dmit)₂]₃ (**1**) at different pressures.

No sign of superconductivity or localization can be detected down to 0.4 K. However, both the conductivity under ambient conditions and the residual resistivity between 300 and 0.4 K (residual resistivity ratios of 15–50) are lower than the values found for compounds where superconductivity is present, for instance, [TTF][Ni(dmit)₂]₂.⁵

3.3. Band-Structure Calculations. The calculation of the band structure using a tight-binding model and including a Coulomb repulsion of at least 0.6 and 0.7 eV for **1** and **2**, respectively, showed that the conduction band of both compounds is HOMO derived.

Figure 7 shows the schemes of intermolecular orbital overlap integrals in the *bc* plane of **1** and the *ab* plane of **2**. The values of the integrals are listed in Table 6. For **1**, relatively large

overlap integrals are found in all directions, including the intersheet *a* direction. These large integrals explain the reasonably high room-temperature conductivity. At the same time, the continuous high overlap in all three dimensions of the compound should also prohibit the occurrence of a Peierls distortion at lower temperatures, which is in perfect agreement with the measured metallic conductivity down to low temperature.

As stated in section 3.1, the difference between the modes of intermolecular overlapping and the distance between the units in the stack of **2** (Figure 4b) results in a rather large difference in the overlap integrals *A* and *B*. This explains the semiconducting behavior of the compound. The fact that no short S···S interactions were found in the intersheet *c* direction explains why the overlap integrals in that direction are very low.

Figure 8 shows the band structures of the two compounds. As the number of Ni(dmit)₂ units in the unit cell is 12 for **1**, 12 HOMO and 12 LUMO bands are presented in Figure 8a. The bands show a reasonable to high dispersion in all directions, indicating a three-dimensional electronic structure. Figure 8b represents the three bands of the HOMO and the LUMO of the three Ni(dmit)₂ units in the unit cell of **2**. There is almost no dispersion in the MR direction, giving the structure a two-dimensional character.

The Fermi level for **1**, for *U* > 0.6 eV, crosses several of the HOMO bands. Therefore, no energy gap is present, and the compound should be a metallic conductor with a one-third-filled conduction band. This metallic conductivity agrees with the results of the conductivity measurements. The Fermi level for **2**, for *U* > 0.7 eV, shows that this compound should be a semiconductor with an activation energy of 0.040 eV, as the Fermi level lies just between two levels. The semiconducting behavior was also found in the conductivity measurements, albeit with an activation energy of 0.11 eV. Such a deviation is not uncommon in a calculation of an activation energy. For comparison, the Fermi levels are also shown for *U* = 0, *i.e.* when Coulomb repulsion is neglected. In this case, both compounds are calculated to be metallic conductors. For **2**, this result does not agree with the results of the conductivity measurements, showing that the inclusion of Coulomb repulsion is important to obtain reliable results of a band-structure calculation.

The relative conductivity of both compounds was calculated from the bandwidth (*W*) and the activation energy (*E_a*) of the band structures.¹⁹ Formula 1 was used with a relativity constant

$$\sigma \propto W e^{E_a/kT} \quad (1)$$

of 3.13×10^{21} . As **1** is a metallic conductor, an activation energy of 0 eV was used, and as there is no conduction by holes in a metallic conductor, the value calculated by formula 1 should be divided by 2. For a bandwidth of 0.125 eV, this results in a calculated conductivity of $31 \text{ S}\cdot\text{cm}^{-1}$, slightly smaller than the measured value for the three crystals, but of the same order of magnitude. Compound **2** contains a direct band gap with an activation energy of 0.040 eV and calculated bandwidths of 0.011 eV for the electrons and 0.040 eV for the holes. For the calculation of the conductivity, the average value of 0.0255 eV was used, resulting in a relative conductivity of $2.6 \text{ S}\cdot\text{cm}^{-1}$, similar to the measured value of $4 \text{ S}\cdot\text{cm}^{-1}$.

4. Discussion and Concluding Remarks

The characterization of **1** shows that a planar cation can increase the dimensionality of a Ni(dmit)₂ compound enor-

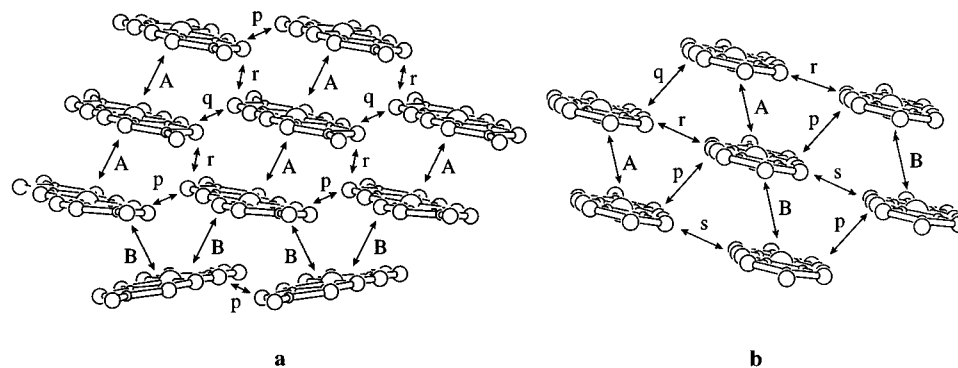


Figure 7. Schemes of the intermolecular orbital overlap integrals of the HOMOs of the Ni(dmit)₂ units of (a) [AcrH][Ni(dmit)₂]₃ (**1**) and (b) [PheH][Ni(dmit)₂]₃ (**2**).

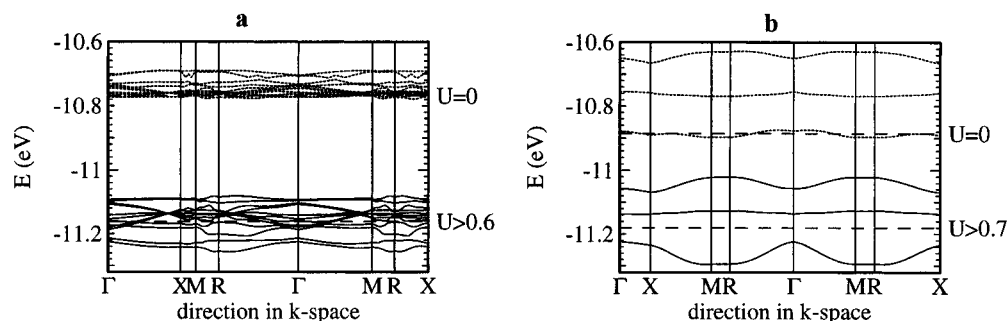


Figure 8. Band structures of (a) [AcrH][Ni(dmit)₂]₃ (**1**) and (b) [PheH][Ni(dmit)₂]₃ (**2**), calculated without Coulomb repulsion ($U = 0$). The symbols Γ , X, M, and R along the horizontal axis correspond with the wave vectors $(0, 0, 0)$, $(\pi/a, 0, 0)$, $(\pi/a, \pi/b, 0)$, and $(\pi/a, \pi/b, \pi/c)$, respectively, with a , b , and c being the lengths of the basis vectors of the unit cells. The solid lines indicate the HOMO-derived bands; the dotted lines, LUMO-derived bands. The upper dashed line indicates the Fermi level for $U = 0$. The conduction band is now LUMO derived. For $U > 0.6/0.7$ eV, the Fermi level is given by the lower dashed line. The energies along the vertical axes should then be shifted by $U/2$. From the figure one can see that the conduction bands are now HOMO derived.

Table 6. Absolute Values ($\times 10^4$) of the Intermolecular Orbital Overlap Integrals of the HOMOs of the Ni(dmit)₂ Units, Defined in Figure 7

compd	A	B	p	q	r	s	intersheet direction
1	12.3	11.2	15.2	14.3	30.1		$\left\{ \begin{array}{l} 17.6 \\ 0.9 \end{array} \right.$
2	92.2	6.5	44.7	72.9	21.3	10.7	$\left\{ \begin{array}{l} 0.2 \\ 0.5 \end{array} \right.$

mously. Short S \cdots S interactions are found in all three dimensions, and the shortest interaction is even found in the intersheet direction, the direction in which often no contacts are found at all. The high dimensionality is also found in the band structure and agrees with the fact that **1** is a metallic conductor down to 4 K; *i.e.*, no Peierls distortion occurs.

The spanning overlapping mode, as found in **1**, has been found previously in two other compounds, α -[Et₂Me₂N]-[Ni(dmit)₂]₂ and [N,N-dimethylpiperidinium][Ni(dmit)₂]₂.^{37,38} These compounds are metallic conductors down to low temperature as well and do not become superconducting under high pressure. Apparently, the spanning overlapping mode results in such a metallic conductivity behavior. Unfortunately, the large difference between the three cations of the spanning overlapping compounds does not provide any clue as to how to synthesize more of these compounds.

The agreement between the conductivity measurements and the band-structure calculations shows that the model applied for the series of [Me_x-guanidinium][Ni(dmit)₂]₂ compounds ($x = 0, 2, 4, 6$) is also applicable for these compounds. It was again shown that the inclusion of Coulomb repulsion is important to obtain reliable results for the theoretical calculations.

The difference in crystal structure, and therefore in conducting properties, observed upon replacing one CH group of acridinium in **1** by a N atom in phenazinium in **2** may seem unexpected. However, the compounds have been synthesized by two completely different methods; **1** was synthesized by electro-oxidation of [AcrH][Ni(dmit)₂] and **2** by interdiffusion of solutions of [Bu₄N][Ni(dmit)₂] and PheHBF₄. It is known that a small change, such as *e.g.* the thickness of the electrodes (and therefore the current density) during the electro-oxidation, can already result in a polymorphic form.^{39,40} The use of the different methods of synthesis may therefore explain the difference in crystal structure between the compounds.

A remarkable resemblance between the compounds is the anion:cation ratio of 3. Only a few Ni(dmit)₂ compounds with this ratio are known, for instance, with tetraphenylphosphonium⁴¹ or cobaltocenium⁴² as a counterion. Consideration of ratios of 3.5 with Bu₄N⁺ and 4 with tetraphenylarsenium⁴³ as counterions, leads to the impression that a larger cation results in a larger ratio. This conclusion may be an important step forward in understanding the packing of the partially oxidized Ni(dmit)₂ compounds. Future work will deal with variations in the synthetic method and with even larger counterions.

(39) Cornelissen, J. P.; Müller, E.; Vaassens, P. H. S.; Haasnoot, J. G.; Reedijk, J.; Cassoux, P. *Inorg. Chem.* **1992**, *31*, 2241.

(40) (a) Gavezotti, A. *Acc. Chem. Res.* **1994**, *27*, 309. (b) Dunitz, J. D.; Bernstein, J. *Acc. Chem. Res.* **1995**, *28*, 193.

(41) Nakamura, T.; Underhill, A. E.; Treeve Coomber, A.; Friend, R. H.; Tajima, H.; Kobayashi, A.; Kobayashi, H. *Inorg. Chem.* **1995**, *34*, 870.

(42) Faulmann, C.; Delpech, F.; Malfant, I.; Cassoux, P. *J. Chem. Soc., Dalton Trans.* **1996**, 2261.

(43) Valade, L.; Legros, J.-P.; Cassoux, P.; Kubel, F. *Mol. Cryst. Liq. Cryst.* **1986**, *140*, 335.

Acknowledgment. Dr. H. B. Brom is thanked for fruitful discussions about the band-structure calculations. This work was supported in part (A.L.S., W.J.J.S, and N.V.) by the Netherlands Foundation of Chemical Research (SON) with financial aid from the Netherlands Organization for Scientific Research (NWO) and in part (Y.S.J.V.,P.M.P., J.G.H., J.R.) by the WFMO (Werkgroep Fundamenteel Materialen Onderzoek of Leiden University). Financial support by the European Community, allowing exchange of preliminary results with several European

colleagues, under Contract ERBCHRXCT920080 is gratefully acknowledged.

Supporting Information Available: Listings of data collection and refinement details, atomic coordinates including those for hydrogen atoms, all anisotropic thermal parameters, all bond lengths and angles, and all S···S interactions for **1** and **2** (16 pages). Ordering information is given on any current masthead page.

IC970347B